A Modular One-Pot Strategy for the Synthesis of Heterobivalent Tracers

Thibaud Bailly, Sacha Bodin, Victor Goncalves, Franck Denat, Clément Morgat, Aurélie Prignon, Ibai E Valverde

▶ **To cite this version:**

Thibaud Bailly, Sacha Bodin, Victor Goncalves, Franck Denat, Clément Morgat, et al.. A Modular One-Pot Strategy for the Synthesis of Heterobivalent Tracers. ACS Medicinal Chemistry Letters, In press, 10.1021/acsmedchemlett.3c00057 . hal-04087376

HAL Id: hal-04087376
https://hal.science/hal-04087376

Submitted on 3 May 2023

HAL is a multi-disciplinary open access archive for the deposit and dissemination of scientific research documents, whether they are published or not. The documents may come from teaching and research institutions in France or abroad, or from public or private research centers.

L'archive ouverte pluridisciplinaire **HAL**, est destinée au dépôt et à la diffusion de documents scientifiques de niveau recherche, publiés ou non, émanant des établissements d'enseignement et de recherche français ou étrangers, des laboratoires publics ou privés.

A modular one-pot strategy for the synthesis of heterobivalent tracers

Thibaud Bailly,[a] Sacha Bodin,[b] Victor Goncalves,[a] Franck Denat,[a] Clément Morgat,[b][c] Aurélie Prignon,[d] Ibai E. Valverde*[a]

[a] Institut de Chimie Moléculaire de l'Université de Bourgogne, UMR CNRS 6302, Université de Bourgogne, 21000 Dijon, France

[b] University of Bordeaux, CNRS, EPHE, INCIA, UMR 5287, Bordeaux F-33000, France

[c] Nuclear Medicine Department, University Hospital of Bordeaux, Bordeaux F-33000, France

[d] UMS28 Laboratoire d'Imagerie Moléculaire Positonique (LIMP), Sorbonne Université, Paris 75020, France

*Email : ibai.valverde@u-bourgogne.fr

Abstract

Bivalent ligands, *i.e.*, molecules having two ligands covalently connected by a linker, have been gathering attention since the first description of their pharmacological potential in the early 80s. However, their synthesis, particularly of labeled heterobivalent ligands, can still be cumbersome and time-consuming. We herein report a straightforward procedure for the modular synthesis of labeled heterobivalents ligands (HBLs) using dual reactive 3,6-dichloro-1,2,4,5-tetrazine as a starting material, and suitable partners for sequential S_NAr and inverse electron demand Diels-Alder (IEDDA) reactions. This assembly method conducted in a stepwise or in a sequential one-pot manner, provides a quick access to multiple HBLs. A conjugate combining ligands towards the Prostate-Specific Membrane Antigen (PSMA) and the Gastrin-Releasing Peptide Receptor (GRPR) was radiolabeled and its biological activity was assessed *in vitro* and *in vivo* (receptor binding affinity, biodistribution, imaging) as an illustration that the assembly methodology preserves the tumor targeting properties of the ligands.

Keywords

Bioconjugation, Click chemistry, Drug delivery, Heterobivalent ligands, Radiopharmaceuticals

Letter

Bivalent ligands have been defined as "molecules having two pharmacophores covalently connected by a linker".[1] This category of compounds has been used to design new ligands for various G-protein coupled receptors (GPCR) including the opioid,[1,2], cannabinoid,[3] chemokine,[4] or melanocortin receptor systems among others.[5] One of the interests of heterobivalent ligands (HBLs) resides in the fact that the combination of two ligands for two different receptors may lead to improved pharmacological properties.[6–9] The improvement of the pharmacological properties of bivalent ligands can arise from an increased affinity of the ligand for tissues or cells co-expressing the receptors that the HBLs are aimed at. This could be due to the fact that the binding of a first ligand to its corresponding receptor might bring the second ligand close to its targeted receptor thus increasing its local concentration and its possibility of binding to its corresponding receptor simultaneously or even after dissociation from the first receptor.[8,10] In addition, since some biomarkers may have different expression profiles depending on the individual or within an individual (heterogeneity) or the stage of a disease (change in receptor expression level), HBLs allow to target a larger number of clinical cases with one single molecule.

HBLs find a particularly adequate application in nuclear imaging and therapy of tumors. This is due to the fact that tumors overexpress different receptors thus making multireceptor targeting a way of gaining specificity in tumor targeting.[11] HBL-based radiotracers are expected to display increased uptake in disease tissue, and improved tumor/background ratios at later timepoints.[12,13] A number of receptors such as regulatory peptide receptors, chemokine and integrin receptors,[14,15] among others, have been identified at the surface of tumor cells and could be used for multireceptor targeting.[11,16] An example for such multireceptor expression by tumor

cells can be found in prostate cancer (PCa). Prostate specific membrane antigen (PSMA) is overexpressed in the vast majority of malignant tumors with PSMA expression level increasing with higher tumor stage and grade.[17] The gastrin releasing peptide receptor (GRPR) is also overexpressed by PCa cells and much effort has been dedicated to the development of GRPR-seeking imaging agents.[18,19] However, recent studies have shown that both receptors are differently overexpressed and that GRPR is strongly upregulated in the majority of PCa cases particularly on lower grade whereas higher grade express abundantly the PSMA.[20,21]

In the context of tumor targeting, where antibodies or peptides can be used for imaging and therapy, the generation of peptide-based HBLs is by far easier than the generation of antibody fragment-based HBL conjugates. Furthermore, peptide conjugates benefit from fast diffusion into the tumor, fast clearance from the body, and their use as dimers or multimers tends to increase their *in vivo* half-life.[22,23] A downside of this class of compounds is the importance of the distance separating the two ligands. As a matter of fact this distance requires to be optimized to maximize the benefits of ligand heterobivalency,[2,4,12,24,25] implying the synthesis of libraries of compounds with varied spacer length and nature. With the increased interest of medicinal chemists and radiopharmacists in HBLs, it is of prime importance to provide easy and straightforward procedures to synthesize them. The efficient synthesis of unlabeled HBLs might be performed by linear, sequential or convergent synthesis. However, the use of HBLs as imaging probes requires the addition of an imaging probe, and adds another layer of complexity to the chemical synthesis process. The use of a third polyfunctional molecular entity like a probe (chelator for nuclear imaging or therapy, or an organic-based fluorophore for cellular microscopy or fluorescence imaging) can make classical linear peptide synthesis cumbersome due to the use

of multiple orthogonal protective groups, tedious deprotection and coupling steps that require intermediate purifications, the need of manipulating fully-protected peptides, which can lead to solubility problems, or the inherent instability of some reporter probes (such as organic fluorophores) in classical SPPS conditions.

Developing modular strategies to synthesize radiolabeled HBLs is particularly important since these molecules often need to be optimized to maximize the interactions of the ligands with receptors.[4,12,25,26] The use of a multifunctional molecular scaffold or template is a highly efficient strategy to put together elaborated building blocks. Moreover, when those building blocks are delicate or difficult to synthesize, it is highly desirable that they are incorporated onto the scaffold *via* orthogonal click reactions.[27]

Some amino acids, like lysine, are natural trifunctional platforms that can be advantageously functionalized with orthogonally reactive bioconjugation moieties.[28] Similarly, trifunctionalized benzene rings can also be used as a starting material to provide a useful scaffold.[29] However, both options require multiple modifications of commercial compounds to decorate the chosen scaffold with orthogonally reactive moieties.[30] Alternatively, trichloro 1,3,5-triazines have been noticed as a way to obtain clickable platforms from a readily available commercial substrate.[31] However, the high reactivity of triazines makes them vulnerable to hydrolysis and a large range of nucleophiles (including amines) and therefore requires careful optimization and chemical expertise in its handling.[29,32]

We have recently demonstrated that the use of disubstituted tetrazines bearing various chelating agents and fluorescent organic dyes was a promising way for the effective synthesis of antibody-based multimodal imaging probes.[33–35] To demonstrate both utility and scope of this

approach, we report herein the usefulness of commercial 3,6-dichloro 1,2,4,5-tetrazine (dichloro-*s*-tetrazine) as a trifunctional platform for the modular and straightforward synthesis of heterobivalent ligands functionalized with an imaging probe. To reach this objective, a series of tetrazines derivatized with different tumor targeting vectors of interest in nuclear medicine were synthesized and reacted with a fluorescent organic dye or a chelator to generate radiolabeled heterobivalent imaging and therapy agents (or precursors thereof) (Figure 1). In an effort to make this methodology even more practical, the previously published stepwise procedure was further improved to be carried out in one-pot.

Thanks to the reactivity of the dichloro-s-tetrazine toward nucleophilic species compared to the monosubstituted chlorotetrazine, non-symmetrical tetrazines can be readily obtained by sequential aromatic nucleophilic substitution (S_NAr) of the chlorine atoms with an amine first, then with a thiol. The first substitution reaction of the chlorine by an amino group leads exclusively to a monochlorotetrazine derivative. This is due to the fact that this substituent dramatically increases the electron density in the aromatic ring yielding to a loss of reactivity of the carbon bearing the second chlorine atom. To perform the second substitution, a stronger nucleophile, such as a thiol, is required and quickly affords a disubstituted tetrazine in good yields.[34] The disubstituted tetrazine is then reacted with a strained alkyne or alkene through an IEDDA reaction. It is worth noticing that the last step, the cycloaddition reaction, is completely chemoselective and is particularly well suited to introduce unprotected chelators or moderately stable organic-based fluorophores (Figure 1).

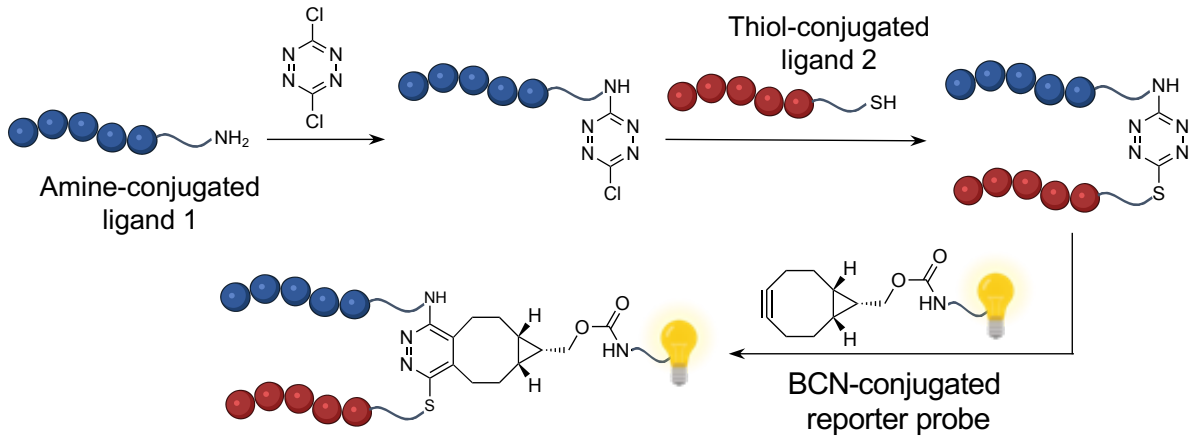

Figure 1. *General principle of the synthesis of heterobivalent ligands using dichloro-s-tetrazine*

Three receptors of interest in tumor imaging were chosen to illustrate the approach, the GRPR, PSMA, and CXCR4, and targeted with compounds **1**, **2**, and **3** respectively (Figure 2). **1** ([DPhe^{6}, Sta^{13}, Leu^{14}]BBN(6-14), also known as JMV594[36]) is a GRPR antagonist displaying nanomolar affinity towards GRPR. It is the targeting moiety of multiple GRPR-seeking radiotracers in clinical trials for prostate and breast cancer.[37] **2** (KuE, lysine-urea-glutamate) is a low molecular weight inhibitor of PSMA. Urea-based PSMA inhibitors have been heavily investigated for their use in nuclear medicine since the mid-2000s,[38] and KuE-based [^{177}Lu]Lu-PSMA-617 (Pluvicto^{TM}) was FDA approved in March 2022 for treatment of progressive, PSMA-positive metastatic castration-resistant PCa. CXCR4 is a chemokine receptor overexpressed in more than 23 cancer types, such as kidney, prostate, lung or brain.[39] **3** (cyclo(DTyr-N(Me)DOrn-Arg-2-Nal-Gly)) is a CXCR4 antagonist exhibiting nanomolar affinity towards the receptor and the targeting moiety of Pentixafor, an imaging agent for CXCR4 in clinical trials for imaging multiple myeloma among other diseases.[40]

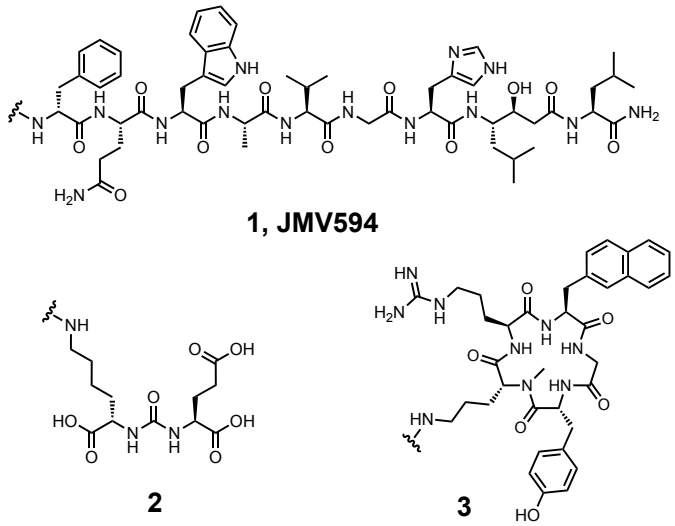

Figure 2. *Structures of targeting moieties **1, 2,** and **3**.*

The vectors were coupled to the tetrazine scaffold *via* spacers of similar length based on β-alanine. Different building blocks were designed depending on the chemical function involved in the coupling reaction with the tetrazine derivative, in this example *N*-Fmoc-$(\beta Ala)_2$-OH **4**, *N*-Boc-$(\beta Ala)_2$-OH **5**, or 3-(3-(tritylthio)propanamido)propanoic acid **6** were used (Figure 3). Compounds **4**, **5**, and **6** were synthesized from the corresponding amine and carboxylic acid using TSTU as a coupling reagent (see supporting information).

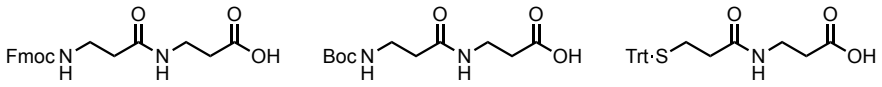

Figure 3*. Structures of different spacers used in the synthesis.*

Prior to reaction with dichloro-s-tetrazine, thiol-substituted **7** was obtained by standard Fmoc/tBu solid-phase peptide synthesis (SPPS) (Scheme 1, see SI for synthesis details). Amino-functionalized **KuE** was obtained by peptide coupling of $KuE(tBu)_3$ **8** with **4** using HATU as a coupling reagent to provide **9** after Fmoc deprotection (Scheme 1). *tris*-tBu ester **9** had to be used since we noticed that dichloro-s-tetrazine was able to react with both amines and carboxylates.

Amino- and thiol- derivatives of compound **3** were synthesized by coupling of **10** with **5** or **6** to provide after deprotection the desired CXCR4-targeting moieties **11** and **12** (Scheme 1).

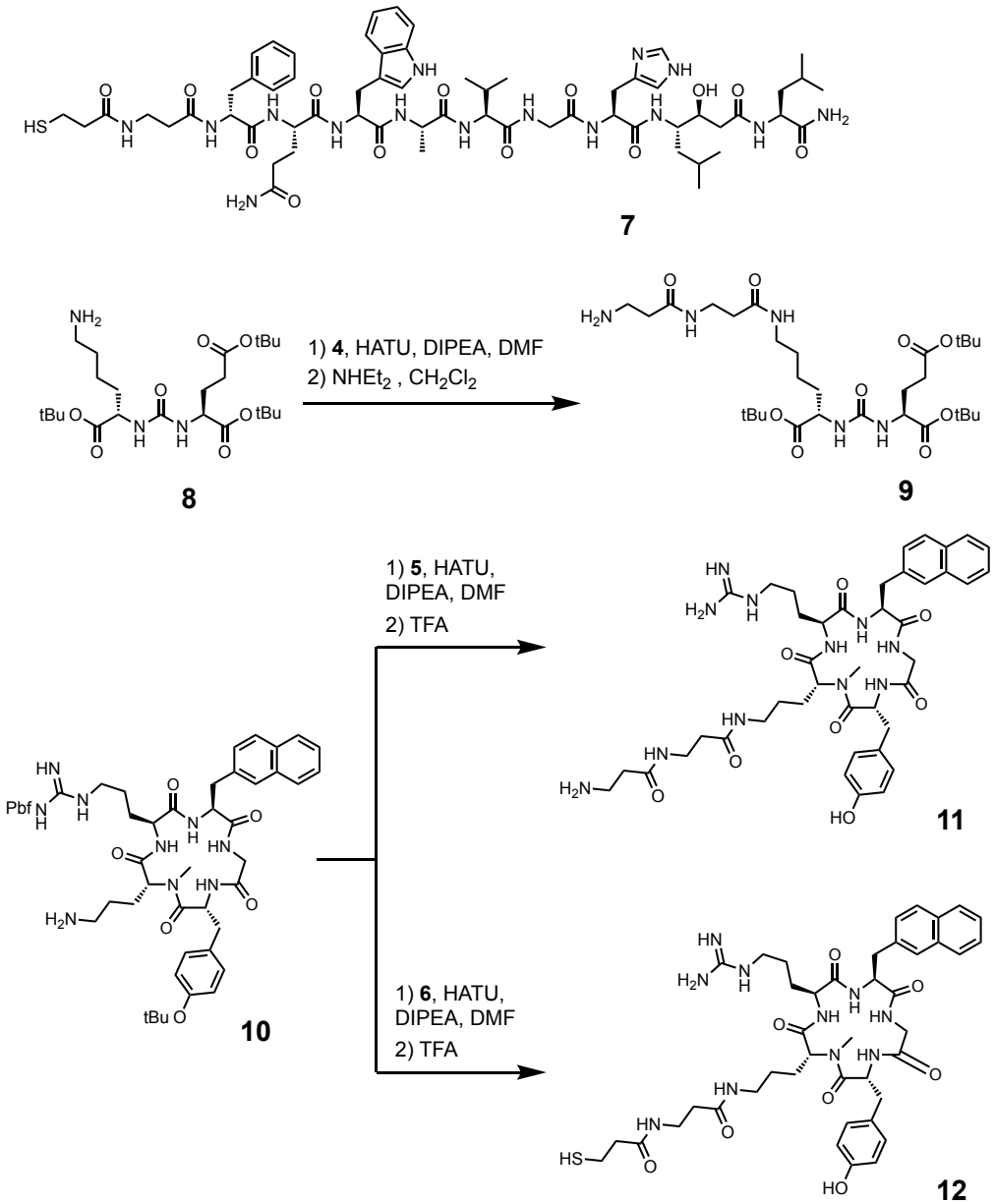

Scheme 1. *Synthetic reactions used for the preparation of thiol- and amino-functionalized CXCR4, GRPR, and PSMA ligands.*

The procedure to generate heterobivalent ligands was as follows: amino-functionalized vectors **9** or **11** were reacted with at least 1 equivalent of dichloro-s-tetrazine in DMF in the presence of DIPEA for 10 minutes. The reaction mixture was then purified by RP-HPLC to yield

chlorotetrazines **13** and **14**. It is worth noting that mono-chlorotetrazines can be prone to hydrolysis, thus they must be stored at -20 °C or immediately used in the next step (Scheme 2). Additionally, it is important to stress the fact that the first substitution is not chemospecific and dichloro-s-tetrazine will react with amines or thiols but also with mild nucleophiles such as carboxylates, leading to the formation of mono-carboxytetrazines,[41] which will afford hydroxytetrazines after spontaneous hydrolysis. Amines were chosen as the first reactive partner since substitution with an amine deactivates significantly the tetrazine core towards the next substitution; whereas a first substitution with a thiol might result in disubstituted compounds if stoichiometry is not carefully controlled.

The thiol-functionalized **7** or **12** were then reacted with the isolated mono-substituted chlorotetrazine in DMF using DIPEA as a base (Figure 4b). As an illustration of the deactivation of the chlorotetrazine, the second substitution must be performed at high temperature (80 °C) and yielded the disubstituted tetrazine in 4 h (Figure 4c). After completion of the reaction, a BCN-derivatized probe (1.2 - 3 equivalents) was added to the reaction and stirred overnight at 37 °C to afford an HBL functionalized with a far-red fluorescent dye (Cy5) or different chelators for labeling with radiometals for diagnosis and therapy (DOTA, NODAGA) in yields ranging from 4% to 40% (Scheme 2). In the case of the cycloaddition, a higher reaction concentration resulted in shorter reaction times (Table 1, lines 2 and 6). Interestingly, the reaction could be performed at concentrations as low as 4 mM affording the target compounds in moderate yields (Table 1, lines 1 and 5). In these cases, the use of an excess of alkyne was preferred. The lowest synthetic yield was achieved with compound **20** which can be explained by the use of the acid-sensitive Cy5 fluorescent dye. The replacement of TFA with formic acid for the cleavage of *tert*-butyl esters led

to partial formylation of the peptide moiety. Subsequent treatment of the crude mixture with aqueous ammonia allowed the obtention of the target compound (see Supporting Information). All these additional treatments, an additional purification, along with the sensitivity of the Cy5 seem to lead to a low yield.

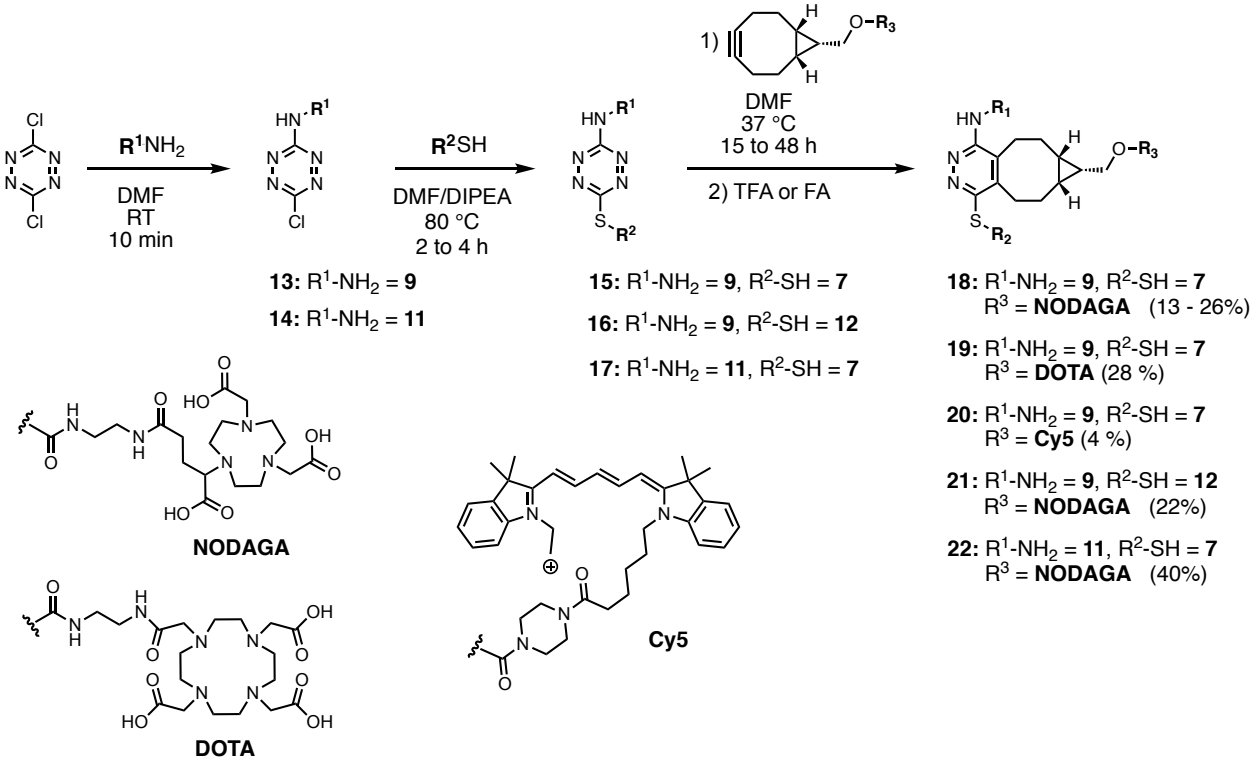

Scheme 2. *General synthetic route towards HBL-based imaging agents. Overall yields (with intermediate purifications of* ***13*** *and* ***14****) are indicated in parentheses. TFA was used to deprotect compounds* ***18****,* ***19****,* ***21****, and* ***22*** *whereas FA was preferred for compound* ***20****.*

Table 1. *Summary of reaction conditions used for the synthesis of compounds* ***18*** *to* ***22***

	Cpd.	Method	Precursor	Reporter probe	Concentration (mM)	Yield (%)
1	**18**	Sequential	**15** 3.8 μmol	BCN-NODAGA 3.1 equiv.	8	13
2	**18**	One pot	**15** 11.1 μmol	BCN-NODAGA 2.7 equiv.	46	26
3	**19**	Sequential	**15** 9.6 μmol	BCN-DOTA 1.8 equiv.	14	28

4	**20**	Sequential	**15** 10 μmol	BCN-Cy5 1.2 equiv.	10	4
5	**21**	Sequential	**16** 0.37 μmol	BCN-NODAGA 3.8 equiv.	4	22
6	**22**	Sequential	**17** 4.7 μmol	BCN-NODAGA 1.4 equiv.	47	40

To increase the potency of this method, we have developed a one-pot version of this procedure which allowed to avoid several intermediate purifications and lyophilizations, saving time and increasing the overall yield. In order to validate the one pot strategy, HBL **18** was resynthesized and obtained in 26% yield (*vs*. 13% with a stepwise procedure). The analytical traces of each synthetic step have been provided in Figure 4 to show the efficiency of each reaction (Figure 4).

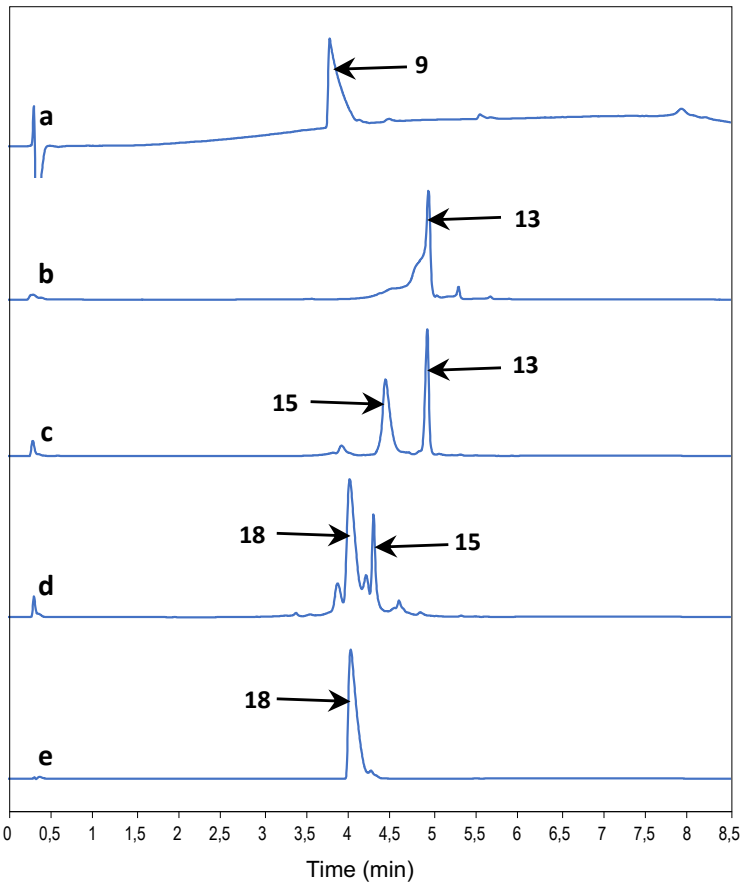

Figure 4. *Representative chromatograms of the crude mixture at different steps of the one-pot synthesis of* ***18****. a) Chromatogram of* ***9****, b) chromatogram of the crude mixture of the reaction the reaction* ***9*** *with dichlorotetrazine to provide* ***13****, c) chromatogram of the crude mixture of* ***13*** *after 2.5 h reaction with* ***7*** *to yield* ***15****, d) chromatogram of the one pot synthesis of* ***15*** *after 20 h reaction with BCN-NODAGA, e) chromatogram of* ***18*** *after final purification. Vertical axis represents relative absorbance at 260 nm with the exception of a) that was recorded at 214 nm due to the lack of absorbance of* ***9*** *at 260 nm. See Supporting Information for detailed information on gradient and analytical system.*

In addition to being beneficial in terms of time – the synthesis of a HBL can be performed in less than 24 hours – the one-pot procedure is also efficient as it resulted in a threefold increase in yield. This methodology was successfully exemplified with the synthesis of other monovalent and heterobivalent conjugates (see Supporting Information).

In order to illustrate the fact that the assembly methodology provides fully functional conjugates without hampering the interaction of the ligands with their receptor, we set out to evaluate the tumor targeting properties of conjugate **18** *in vivo*.

Compounds were radiolabeled with [^{68}Ga]$GaCl_3$ in sodium formate buffer (6.6 mg, pH 3.5) for 10 min at 40 °C (**18** and **PSMA 11**) or at 95°C (**AMBA**) . The radioconjugates were purified on a C18 Sep-Pak cartridge to achieve radiochemical purities > 98%, as determined by radio-HPLC. Radiochemical yields ranged from 79% to 95% (not optimized). Molar activities were 12.7 ± 6.1 MBq/nmol for *in vitro* studies and ranged from 2.44 to 10.94 MBq/nmol for *in vivo* studies. For *in vivo* experiments, radiolabeling, quality control and intravenous injection were performed within 1 h. **PSMA 11** and **AMBA** were used as standards for validation of the PSMA and GRPR double xenografts *in vivo*.[42]

Distribution coefficient at pH 7.4 (logD) of [^{68}Ga]Ga-**18** was determined by the shake-flask method obtained from saturated octanol-PBS solution (0.1 M, pH 7.4). The radiolabeled tracer exhibited a logD of -2.47 ± 0.19 which is typical of peptide-based tracers and can be attributed to the presence of several hydrophilic groups such as carboxylate groups and amide bonds.

Saturation binding experiments of [^{68}Ga]Ga-**18** towards GRPR and PSMA were determined on PC3 cells ($PSMA^-/GRPR^+$) and 22Rv1 cells ($GRPR^-/PSMA^+$). A K_D value of 1.9 ± 1.2 nM towards the GRPR was obtained on PC3 cells and value of 17.7 ± 4.9 nM towards the PSMA was obtained on 22Rv1 cells (22Rv1 express a small amount of GRPR, in this case GRPR interaction was blocked by co-incubation with 10 µM of bombesin). Affinity of [^{68}Ga]Ga-**18** towards the GRPR and the PSMA were lower than GRPR- and PSMA-targeting standards such as [^{68}Ga]Ga-RM2 (K_D = 0.3 ± 0.2 nM

on PC3 cells),[43] and [^{68}Ga]Ga-PSMA-617 (K_i = 2.3 ± 2.9 nM on LnCaP cells)[44] but still in the nanomolar range.[44]

To assess [^{68}Ga]Ga-**18** *in vivo,* a model of athymic nude mice doubly-xenografted with PC3 cells on the left shoulder and 22Rv1 cells on the right shoulder was used.[42] To validate the model, two well-established radioligands of PSMA and GRPR, respectively [^{68}Ga]Ga-**PSMA11** (1.18 nmol, 7.67 MBq) and [^{68}Ga]Ga-**AMBA** (763 pmol, 5.41 MBq), were injected through retro-orbital injection.

Images recorded 50-70 min post injection (p.i.) showed that both tracers were able to exclusively accumulate in the xenograft overexpressing their complementary receptor which demonstrated uptake specificity (3.46 % ID/g for [^{68}Ga]Ga-**AMBA** in PC3 tumor and 3.22 % ID/g for [^{68}Ga]Ga-**PSMA11** in 22Rv1 tumor, Figure 5). Both radioconjugates show uptake in the kidneys, which is typical of peptide-based radiotracers that, with few exceptions, benefit from renal excretion. [^{68}Ga]Ga-**AMBA** shows uptake in the gastrointestinal tract which is due to the presence of GRPR in the pancreas, stomach and colon.[45]

At only 30-50 min p.i., [^{68}Ga]Ga-**18** (1.88 nmol, 4.1 MBq) already showed accumulation in targeted tumor xenografts with 1.76 % ID/g for PC3; 1.66 % ID/g for 22Rv1 (measured by quantitative PET imaging, see supporting information) and GRPR or PSMA-positive tissues such as pancreas and kidneys (Figure 5, right). Quantitative PET measurements 20 min later did not show additional accumulation in both tumors (1.75 % ID/g for PC3; 1.69 % ID/g for 22Rv1). A significant decrease in the signal from the blood pool (1.02 % ID/g for heart), showing circulation of the radiotracer and washout from the background let us anticipate an improved contrast at later timepoints in comparison with the images at 30-50 min (Figure 5). Most signal was observed in

the kidneys and in the bladder, suggesting that [^{68}Ga]Ga-**18** is eliminated mainly through renal/urinary excretion. A weak signal in the gallbladder and high background in the abdominal region suggested a small amount of hepatobiliary excretion. The uptake of [^{68}Ga]Ga-**18** in each xenograft (1.75 and 1.69 % ID/g in PC3 and 22Rv1 xenografts) at 50-70 min was lower than the reference compounds (3.46 and 3.22 % ID/g respectively). We hypothesize that this difference might be due to the structure of **18**, that has not been optimized like **AMBA** or **PSMA11**.

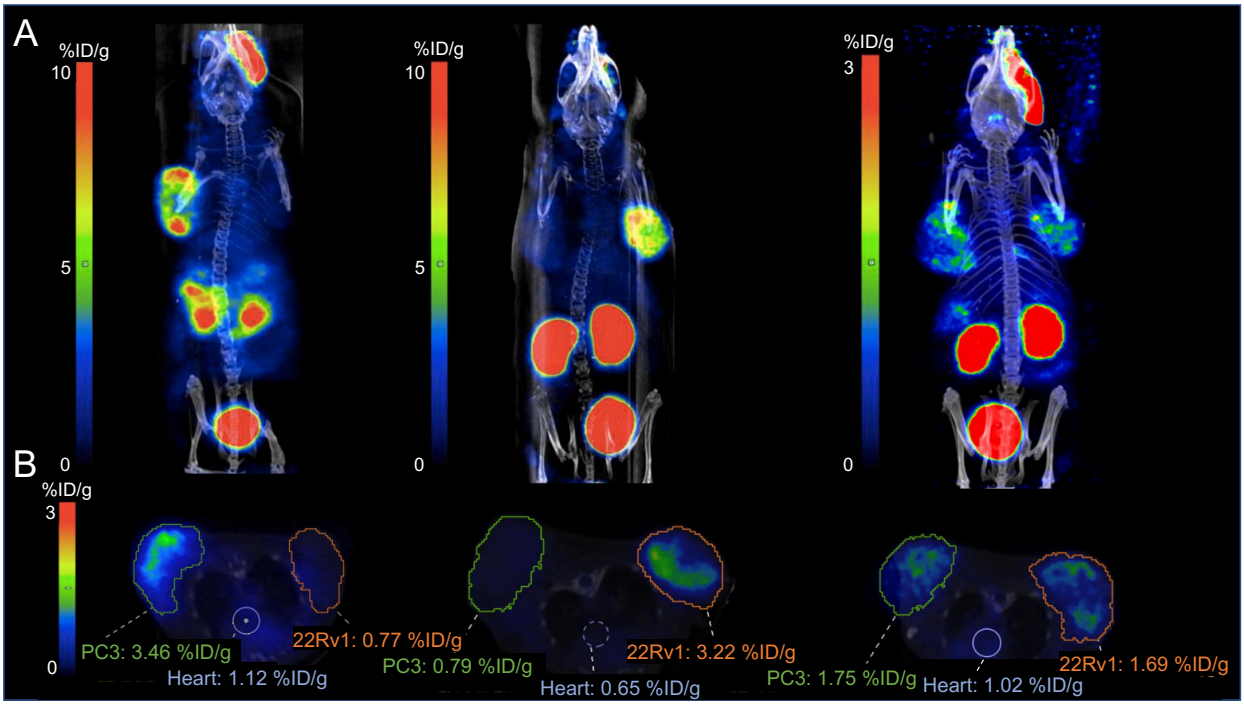

***Figure 5**: (A) The images show the maximum intensity projections recorded between 50-70 min. p.i. of [^{68}Ga]Ga-**AMBA** (A, left) ; [^{68}Ga]Ga-**PSMA11** (A, middle) and [^{68}Ga]Ga-**18** (A, right). (B) The images show the axial images VOI analysis around both PC3 and 22Rv1 tumors, and heart as blood pool background. Signal seen on the head of the mice is due to retro-orbital injection*

These results were confirmed *via* a biodistribution study, performed 2 h p.i.. Uptake specificity was confirmed by blocking experiments. In short, [^{68}Ga]Ga-**18** was injected alone (533 ± 72 pmol), or in combination with a large excess of bombesin (BBN(1-14)) or PMPA (1000 molar equivalents). Mice were euthanized after 2 hours, organs were collected, weighed and the

amount of radioactivity was measured in a γ-counter. Data showed a fast clearance from the blood and radioactivity accumulated in organs positive to PSMA and GRPR (kidneys, pancreas) and the tumor xenografts thus confirming the behavior observed by PET imaging. Blocking of each receptor resulted in a statistically significant decrease of radioactivity in both PC3 and PSMA xenografts, confirming the specificity of the uptake of [^{68}Ga]Ga-**18**. The uptake in the tumors was 1.31 ± 0.11 % ID/g (PC3) and 1.01 ± 0.15 % ID/g (22Rv1) (Figure 6).

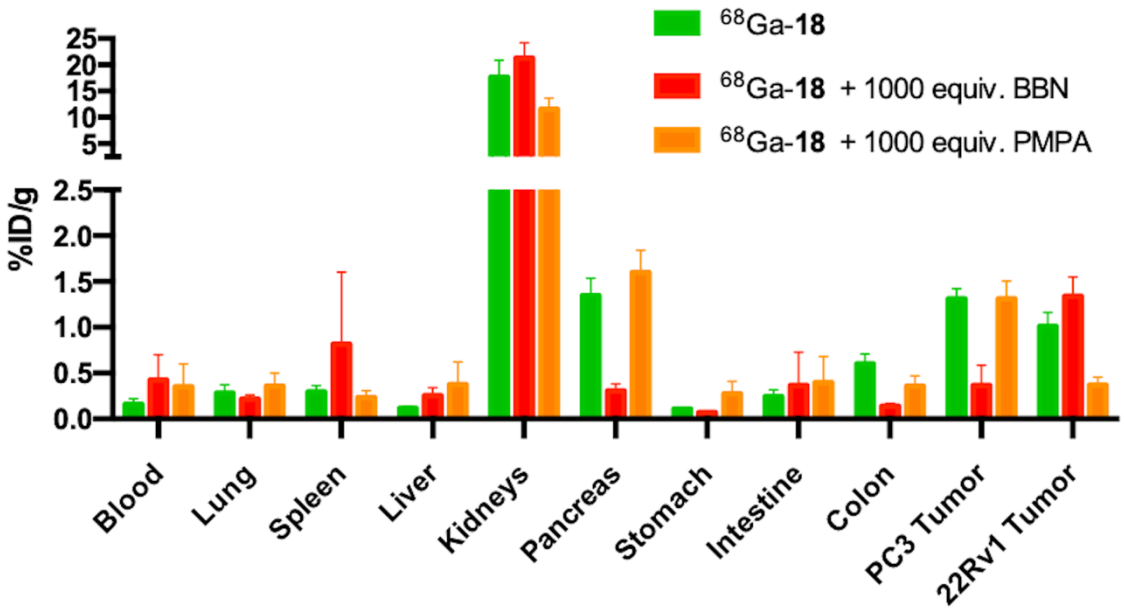

Figure 6*: Biodistribution of [^{68}Ga]Ga-**18** at 2 h p.i. in nude mice xenografted with PC3 and 22Rv1 cells. Data points show mean ± SEM. n = 2-5, for values of all collected tissues and tumor-to-tissue ratios see the supporting information.*

In summary, a straightforward method based on the use of dichloro-s-tetrazine to quickly access labeled heterobivalent ligands has been successfully developed. We have demonstrated that the method is suited to easily assemble thiol- and amino-functionalized peptide-based ligands, and different labels useful for medical imaging. The strategy, based on the use of multiple chemoselective reactions, successfully provided complex molecular structures in a straightforward, time-saving, and modular manner. The efficiency of our procedure has been

further increased by developing a one-pot approach giving three times higher yields in a shorter amount of time than the stepwise approach. To our knowledge, this is the first example of peptide-based heterobivalent ligands for imaging assembled in one pot. *In vitro* and *in vivo* evaluation of the pharmacological properties of one of the conjugates demonstrated that the platform-based assembly method does not hamper the interaction of the ligands with their receptors.

Based on the increasing number of studies on bivalent and heterobivalent ligands, we expect that this methodology will be of interest in the field of drug design, drug delivery, imaging, and peptide receptor radiotherapy.

Supporting information

Synthesis and full characterization of compounds **4** to **22** and [^{68}Ga]**22** (γ-HPLC), examples of other compounds synthesized *via* the one pot procedure, radiolabeling procedures, and experimental protocols of *in vitro* and *in vivo* experiments can be found in the Supporting Information.

Author information

Corresponding Author

* Ibai E. Valverde, Institut de Chimie Moléculaire de L'Université de Bourgogne, UMR 6302, Univ. Bourgogne Franche-Comté, 9, Avenue Alain Savary, 21078, Dijon Cedex, France;

ibai.valverde@u-bourgogne.fr, +33 380 39 90 48

Abbreviations

Ahx, 6-aminohexanoyl ; AMBA, DOTA-G-(4-aminobenzoyl)-QWAVGHLM-NH_2 ; Cpd , compound ; DOTA, 1,4,7,10-tetraazacyclododecane-1,4,7,10-tetraacetic acid ; DIPEA, *N,N*-diisopropylethylamine ; DUPA , 2-[3-(1, 3-dicarboxy propyl)ureido]-pentanedioic acid ; FA, formic acid ; HATU, *O*-(7-azabenzotriazol-1-yl)-*N,N,N',N'*-tetramethyluronium hexafluorophosphate ; HBED-CC, N,N'-di(2-hydroxybenzyl)ethylenediamine-N,N'-diacetic acid ; HR-MS, high-resolution mass spectrometry ; ID, injected dose ; IEDDA , inverse electron-demand Diels-Alder ; NODAGA, (R)-1,4,7-triazacyclononane-1-glutaric acid-4,7-acetic acid ; PMPA, 2-(phosphonomethyl)pentanedioic acid ; PSMA11, HO-Glu-CO-Lys(HBED-CC-Ahx)-OH ; RP-HPLC, reverse-phase high-performance liquid chromatography ; SPPS, solid-phase peptide synthesis ; Sta, statine, (3S,4S) 4-amino-3-hydroxy-6-methylheptanoic acid ; TFA, trifluoroacetic acid ; TSTU, *N,N,N',N'*-tetramethyl-*O*-(*N*-succinimidyl)uronium tetrafluoroborate.

Acknowledgments

This work is part of the project "Pharmacoimagerie et Agents Théranostiques" supported by the Université de Bourgogne and Conseil Régional de Bourgogne through the Plan d'Action Régional pour l'Innovation (PARI), the Région Bourgogne Franche-Comté through the ANER (grant DIPEPT 2018Y-07073) and Excellence programs (grant MULTIMOD), and the European Union through the PO FEDER-FSE Bourgogne 2014/2020 programs. This work was achieved within the frame of the NEWMOON Impulsion of Bordeaux University. This work was also partly funded by France Life Imaging (grant ANR-11-INBS-0006). GDR CNRS "Agents d'Imagerie Moléculaire" 2037 is thanked for its interest in this research. We thank the "Plateforme d'Analyse Chimique et de Synthèse Moléculaire de l'Université de Bourgogne" (PACSMUB, http://www.wpcm.fr) for access to

analytical and molecular spectroscopy instruments. The authors also thank Prof. Anthony Romieu (University of Burgundy, ICMUB) for the gift of bioconjugatable Cy5 and revision of the manuscript, Dr. Quentin Bonnin (CNRS, PACSMUB) and Marie-José Penouilh (University of Burgundy, PACSMUB) for HR-MS analyses, and Dr. Myriam Heydel (University of Burgundy, PACSMUB) for the determination of TFA content in samples purified by semi-preparative RP-HPLC. KuE(tBu)$_3$, NODAGA-BCN, and DOTA-BCN were a generous gift from CheMatech (Dijon, France).

References

(1) Portoghese, P. S.; Ronsisvalle, G.; Larson, D. L.; Yim, C. B.; Sayre, L. M.; Takemori, A. E. Opioid Agonist and Antagonist Bivalent Ligands as Receptor Probes. *Life Sci.* **1982**, *31* (12–13), 1283–1286. https://doi.org/10.1016/0024-3205(82)90362-9.

(2) Portoghese, P. S.; Larson, D. L.; Sayre, L. M.; Yim, C. B.; Ronsisvalle, G.; Tam, S. W.; Takemori, A. E. Opioid Agonist and Antagonist Bivalent Ligands. The Relationship between Spacer Length and Selectivity at Multiple Opioid Receptors. *J. Med. Chem.* **1986**, *29* (10), 1855–1861. https://doi.org/10.1021/jm00160a010.

(3) Huang, G.; Pemp, D.; Stadtmüller, P.; Nimczick, M.; Heilmann, J.; Decker, M. Design, Synthesis and in Vitro Evaluation of Novel Uni- and Bivalent Ligands for the Cannabinoid Receptor Type 1 with Variation of Spacer Length and Structure. *Bioorg. Med. Chem. Lett.* **2014**, *24* (17), 4209–4214. https://doi.org/10.1016/j.bmcl.2014.07.038.

(4) Tanaka, T.; Nomura, W.; Narumi, T.; Masuda, A.; Tamamura, H. Bivalent Ligands of CXCR4 with Rigid Linkers for Elucidation of the Dimerization State in Cells. *J. Am. Chem. Soc.* **2010**, *132* (45), 15899–15901. https://doi.org/10.1021/ja107447w.

(5) Lensing, C. J.; Freeman, K. T.; Schnell, S. M.; Speth, R. C.; Zarth, A. T.; Haskell-Luevano, C. Developing a Biased Unmatched Bivalent Ligand (BUmBL) Design Strategy to Target the GPCR Homodimer Allosteric Signaling (CAMP over β-Arrestin 2 Recruitment) Within the Melanocortin Receptors. *J. Med. Chem.* **2019**, *62* (1), 144–158. https://doi.org/10.1021/acs.jmedchem.8b00238.

(6) Lensing, C. J.; Freeman, K. T.; Schnell, S. M.; Adank, D. N.; Speth, R. C.; Haskell-Luevano, C. An in Vitro and in Vivo Investigation of Bivalent Ligands That Display Preferential Binding and Functional Activity for Different Melanocortin Receptor Homodimers. *J. Med. Chem.* **2016**, *59* (7), 3112–3128. https://doi.org/10.1021/acs.jmedchem.5b01894.

(7) Josan, J. S.; Handl, H. L.; Sankaranarayanan, R.; Xu, L.; Lynch, R. M.; Vagner, J.; Mash, E. A.; Hruby, V. J.; Gillies, R. J. Cell-Specific Targeting by Heterobivalent Ligands. *Bioconjug. Chem.* **2011**, *22* (7), 1270–1278. https://doi.org/10.1021/bc1004284.

(8) Vauquelin, G.; Charlton, S. J. Exploring Avidity: Understanding the Potential Gains in Functional Affinity and Target Residence Time of Bivalent and Heterobivalent Ligands: Exploring Bivalent Ligand Binding Properties. *Br. J. Pharmacol.* **2013**, *168* (8), 1771–1785. https://doi.org/10.1111/bph.12106.
(9) Peschel, A.; Cardoso, F. C.; Walker, A. A.; Durek, T.; Stone, M. R. L.; Braga Emidio, N.; Dawson, P. E.; Muttenthaler, M.; King, G. F. Two for the Price of One: Heterobivalent Ligand Design Targeting Two Binding Sites on Voltage-Gated Sodium Channels Slows Ligand Dissociation and Enhances Potency. *J. Med. Chem.* **2020**, *63* (21), 12773–12785. https://doi.org/10.1021/acs.jmedchem.0c01107.
(10) Vauquelin, G. Simplified Models for Heterobivalent Ligand Binding: When Are They Applicable and Which Are the Factors That Affect Their Target Residence Time. *Naunyn. Schmiedebergs Arch. Pharmacol.* **2013**, *386* (11), 949–962. https://doi.org/10.1007/s00210-013-0881-0.
(11) Reubi, J. C.; Maecke, H. R. Approaches to Multireceptor Targeting: Hybrid Radioligands, Radioligand Cocktails, and Sequential Radioligand Applications. *J. Nucl. Med.* **2017**, *58* (Supplement 2), 10S-16S. https://doi.org/10.2967/jnumed.116.186882.
(12) Kroll, C.; Mansi, R.; Braun, F.; Dobitz, S.; Maecke, H. R.; Wennemers, H. Hybrid Bombesin Analogues: Combining an Agonist and an Antagonist in Defined Distances for Optimized Tumor Targeting. *J. Am. Chem. Soc.* **2013**, *135* (45), 16793–16796. https://doi.org/10.1021/ja4087648.
(13) Liu, Z.; Niu, G.; Wang, F.; Chen, X. 68Ga-Labeled NOTA-RGD-BBN Peptide for Dual Integrin and GRPR-Targeted Tumor Imaging. *Eur. J. Nucl. Med. Mol. Imaging* **2009**, *36* (9), 1483–1494. https://doi.org/10.1007/s00259-009-1123-z.
(14) Chatterjee, S.; Behnam Azad, B.; Nimmagadda, S. Chapter Two - The Intricate Role of CXCR4 in Cancer. In *Advances in Cancer Research*; Pomper, M. G., Fisher, P. B., Eds.; Emerging Applications of Molecular Imaging to Oncology; Academic Press, 2014; Vol. 124, pp 31–82. https://doi.org/10.1016/B978-0-12-411638-2.00002-1.
(15) Jin, H.; Varner, J. Integrins: Roles in Cancer Development and as Treatment Targets. *Br. J. Cancer* **2004**, *90* (3), 561–565. https://doi.org/10.1038/sj.bjc.6601576.
(16) Reubi, J. C.; Waser, B. Concomitant Expression of Several Peptide Receptors in Neuroendocrine Tumours: Molecular Basis for in Vivo Multireceptor Tumour Targeting. *Eur. J. Nucl. Med. Mol. Imaging* **2003**, *30* (5), 781–793. https://doi.org/10.1007/s00259-003-1184-3.
(17) Wright, G. L.; Haley, C.; Beckett, M. L.; Schellhammer, P. F. Expression of Prostate-Specific Membrane Antigen in Normal, Benign, and Malignant Prostate Tissues. *Urol. Oncol. Semin. Orig. Investig.* **1995**, *1* (1), 18–28. https://doi.org/10.1016/1078-1439(95)00002-Y.
(18) Markwalder, R.; Reubi, J. C. Gastrin-Releasing Peptide Receptors in the Human Prostate Relation to Neoplastic Transformation. *Cancer Res.* **1999**, *59* (5), 1152–1159.
(19) Mansi, R.; Nock, B. A.; Dalm, S. U.; Busstra, M. B.; van Weerden, W. M.; Maina, T. Radiolabeled Bombesin Analogs. *Cancers* **2021**, *13* (22), 5766. https://doi.org/10.3390/cancers13225766.
(20) Beer, M.; Montani, M.; Gerhardt, J.; Wild, P. J.; Hany, T. F.; Hermanns, T.; Müntener, M.; Kristiansen, G. Profiling Gastrin-Releasing Peptide Receptor in Prostate Tissues: Clinical

Implications and Molecular Correlates. *The Prostate* **2012**, *72* (3), 318–325. https://doi.org/10.1002/pros.21434.

(21) Schollhammer, R.; Robert, G.; Asselineau, J.; Yacoub, M.; Vimont, D.; Balamoutoff, N.; Bladou, F.; Bénard, A.; Hindié, E.; Clermont-Gallerande, H. H. de; Morgat, C. Comparison of 68Ga-PSMA-617 PET/CT and 68Ga-RM2 PET/CT in Patients with Localized Prostate Cancer Candidate for Radical Prostatectomy: A Prospective, Single Arm, Single Center, Phase II Study. *J. Nucl. Med.* **2022**. https://doi.org/10.2967/jnumed.122.263889.

(22) Daepp, S.; Garayoa, E. G.; Maes, V.; Brans, L.; Tourwe, D. A.; Mueller, C.; Schibli, R. PEGylation of Tc-99m-Labeled Bombesin Analogues Improves Their Pharmacokinetic Properties. *Nucl. Med. Biol.* **2011**, *38* (7), 997–1009. https://doi.org/10.1016/j.nucmedbio.2011.02.014.

(23) Carlucci, G.; Ananias, H. J. K.; Yu, Z.; Hoving, H. D.; Helfrich, W.; Dierckx, R. A. J. O.; Liu, S.; de Jong, I. J.; Elsinga, P. H. Preclinical Evaluation of a Novel 111In-Labeled Bombesin Homodimer for Improved Imaging of GRPR-Positive Prostate Cancer. *Mol. Pharm.* **2013**, *10* (5), 1716–1724. https://doi.org/10.1021/mp3005462.

(24) Bobrovnik, S. A. The Influence of Rigid or Flexible Linkage between Two Ligands on the Effective Affinity and Avidity for Reversible Interactions with Bivalent Receptors. *J. Mol. Recognit. JMR* **2007**, *20* (4), 253–262. https://doi.org/10.1002/jmr.836.

(25) Dobitz, S.; Wilhelm, P.; Romantini, N.; De Foresta, M.; Walther, C.; Ritler, A.; Schibli, R.; Berger, P.; Deupi, X.; Behe, M.; Wennemers, H. Distance-Dependent Cellular Uptake of Oligoproline-Based Homobivalent Ligands Targeting GPCRs-An Experimental and Computational Analysis. *Bioconjug. Chem.* **2020**, *31* (10), 2431–2438. https://doi.org/10.1021/acs.bioconjchem.0c00484.

(26) Handl, H. L.; Vagner, J.; Han, H.; Mash, E.; Hruby, V. J.; Gillies, R. J. Hitting Multiple Targets with Multimeric Ligands. *Expert Opin. Ther. Targets* **2004**, *8* (6), 565–586. https://doi.org/10.1517/14728222.8.6.565.

(27) Beal, D. M.; Jones, L. H. Molecular Scaffolds Using Multiple Orthogonal Conjugations: Applications in Chemical Biology and Drug Discovery. *Angew. Chem. Int. Ed.* **2012**, *51* (26), 6320–6326. https://doi.org/10.1002/anie.201200002.

(28) Clavé, G.; Volland, H.; Flaender, M.; Gasparutto, D.; Romieu, A.; Renard, P.-Y. A Universal and Ready-to-Use Heterotrifunctional Cross-Linking Reagent for Facile Synthetic Access to Sophisticated Bioconjugates. *Org. Biomol. Chem.* **2010**, *8* (19), 4329–4345. https://doi.org/10.1039/c0ob00133c.

(29) Sato, D.; Wu, Z.; Fujita, H.; Lindsey, J. S. Design, Synthesis, and Utility of Defined Molecular Scaffolds. *Organics* **2021**, *2* (3), 161–273. https://doi.org/10.3390/org2030013.

(30) Viault, G.; Dautrey, S.; Maindron, N.; Hardouin, J.; Renard, P.-Y.; Romieu, A. The First "Ready-to-Use" Benzene-Based Heterotrifunctional Cross-Linker for Multiple Bioconjugation. *Org. Biomol. Chem.* **2013**, *11* (16), 2693–2705. https://doi.org/10.1039/c3ob40086g.

(31) Li, H.; Zhou, H.; Krieger, S.; Parry, J. J.; Whittenberg, J. J.; Desai, A. V.; Rogers, B. E.; Kenis, P. J. A.; Reichert, D. E. Triazine-Based Tool Box for Developing Peptidic PET Imaging Probes: Syntheses, Microfluidic Radiolabeling, and Structure–Activity Evaluation. *Bioconjug. Chem.* **2014**, *25* (4), 761–772. https://doi.org/10.1021/bc500034n.

(32) Mitran, B.; Varasteh, Z.; Abouzayed, A.; Rinne, S. S.; Puuvuori, E.; De Rosa, M.; Larhed, M.; Tolmachev, V.; Orlova, A.; Rosenström, U. Bispecific GRPR-Antagonistic Anti-PSMA/GRPR

Heterodimer for PET and SPECT Diagnostic Imaging of Prostate Cancer. *Cancers* **2019**, *11* (9), 1371. https://doi.org/10.3390/cancers11091371.
(33) Canovas, C.; Moreau, M.; Bernhard, C.; Oudot, A.; Guillemin, M.; Denat, F.; Goncalves, V. Site-Specific Dual Labeling of Proteins on Cysteine Residues with Chlorotetrazines. *Angew. Chem. Int. Ed.* **2018**, *57* (33), 10646–10650. https://doi.org/10.1002/anie.201806053.
(34) Canovas, C.; Moreau, M.; Vrigneaud, J.-M.; Bellaye, P.-S.; Collin, B.; Denat, F.; Goncalves, V. Modular Assembly of Multimodal Imaging Agents through an Inverse Electron Demand Diels–Alder Reaction. *Bioconjug. Chem.* **2019**, *30* (3), 888–897. https://doi.org/10.1021/acs.bioconjchem.9b00017.
(35) Renard, E.; Collado Camps, E.; Canovas, C.; Kip, A.; Gotthardt, M.; Rijpkema, M.; Denat, F.; Goncalves, V.; van Lith, S. A. M. Site-Specific Dual-Labeling of a VHH with a Chelator and a Photosensitizer for Nuclear Imaging and Targeted Photodynamic Therapy of EGFR-Positive Tumors. *Cancers* **2021**, *13* (3), 428. https://doi.org/10.3390/cancers13030428.
(36) Llinares, M.; Devin, C.; Chaloin, O.; Azay, J.; Noel-Artis, A. M.; Bernad, N.; Fehrentz, J. A.; Martinez, J. Syntheses and Biological Activities of Potent Bombesin Receptor Antagonists. *J. Pept. Res.* **1999**, *53* (3), 275–283. https://doi.org/10.1034/j.1399-3011.1999.00028.x.
(37) Mansi, R.; Wang, X.; Forrer, F.; Waser, B.; Cescato, R.; Graham, K.; Borkowski, S.; Reubi, J. C.; Maecke, H. R. Development of a Potent DOTA-Conjugated Bombesin Antagonist for Targeting GRPr-Positive Tumours. *Eur. J. Nucl. Med. Mol. Imaging* **2011**, *38* (1), 97–107. https://doi.org/10.1007/s00259-010-1596-9.
(38) Wang, F.; Li, Z.; Feng, X.; Yang, D.; Lin, M. Advances in PSMA-Targeted Therapy for Prostate Cancer. *Prostate Cancer Prostatic Dis.* **2021**. https://doi.org/10.1038/s41391-021-00394-5.
(39) Chatterjee, S.; Behnam Azad, B.; Nimmagadda, S. The Intricate Role of CXCR4 in Cancer. In *Advances in Cancer Research*; Elsevier, 2014; Vol. 124, pp 31–82. https://doi.org/10.1016/B978-0-12-411638-2.00002-1.
(40) Demmer, O.; Frank, A. O.; Hagn, F.; Schottelius, M.; Marinelli, L.; Cosconati, S.; Brack-Werner, R.; Kremb, S.; Wester, H.-J.; Kessler, H. A Conformationally Frozen Peptoid Boosts CXCR4 Affinity and Anti-HIV Activity. *Angew. Chem. Int. Ed.* **2012**, *51* (32), 8110–8113. https://doi.org/10.1002/anie.201202090.
(41) Kamiński, Z. J. 2-Chloro-4,6-Disubstituted-1,3,5-Triazines a Novel Group of Condensing Reagents. *Tetrahedron Lett.* **1985**, *26* (24), 2901–2904. https://doi.org/10.1016/S0040-4039(00)98867-1.
(42) Zhang-Yin, J.; Provost, C.; Cancel-Tassin, G.; Rusu, T.; Penent, M.; Radulescu, C.; Comperat, E.; Cussenot, O.; Montravers, F.; Renard-Penna, R.; Talbot, J.-N.; Prignon, A. A Comparative Study of Peptide-Based Imaging Agents [68Ga]Ga-PSMA-11, [68Ga]Ga-AMBA, [68Ga]Ga-NODAGA-RGD and [68Ga]Ga-DOTA-NT-20.3 in Preclinical Prostate Tumour Models. *Nucl. Med. Biol.* **2020**, *84–85*, 88–95. https://doi.org/10.1016/j.nucmedbio.2020.03.005.
(43) Chastel, A.; Vimont, D.; Claverol, S.; Zerna, M.; Bodin, S.; Berndt, M.; Chaignepain, S.; Hindié, E.; Morgat, C. 68Ga-Radiolabeling and Pharmacological Characterization of a Kit-Based Formulation of the Gastrin-Releasing Peptide Receptor (GRP-R) Antagonist RM2 for Convenient Preparation of [68Ga]Ga-RM2. *Pharmaceutics* **2021**, *13* (8), 1160. https://doi.org/10.3390/pharmaceutics13081160.
(44) Benešová, M.; Schäfer, M.; Bauder-Wüst, U.; Afshar-Oromieh, A.; Kratochwil, C.; Mier, W.; Haberkorn, U.; Kopka, K.; Eder, M. Preclinical Evaluation of a Tailor-Made DOTA-Conjugated

PSMA Inhibitor with Optimized Linker Moiety for Imaging and Endoradiotherapy of Prostate Cancer. *J. Nucl. Med.* **2015**, *56* (6), 914–920. https://doi.org/10.2967/jnumed.114.147413.

(45) Lantry, L. E.; Cappelletti, E.; Maddalena, M. E.; Fox, J. S.; Feng, W.; Chen, J.; Thomas, R.; Eaton, S. M.; Bogdan, N. J.; Arunachalam, T.; Reubi, J. C.; Raju, N.; Metcalfe, E. C.; Lattuada, L.; Linder, K. E.; Swenson, R. E.; Tweedle, M. F.; Nunn, A. D. 177Lu-AMBA: Synthesis and Characterization of a Selective 177Lu-Labeled GRP-R Agonist for Systemic Radiotherapy of Prostate Cancer. *J. Nucl. Med.* **2006**, *47* (7), 1144–1152.

TOC graphic